C5-1471.4/3111 Copy 73

PROCESS TECHNIQUES STUDY OF INTEGRATED CIRCUITS

Quarterly Report No. 4

May 15, 1966

Prepared by:

J. E. Meinhard

AUTONETICS

A DIVISION OF NORTH AMERICAN AVIATION, INC.

Prepared Under Contract

NAS 12-4

General Order 6433

Approved by:

P. H. Eisenberg

P. H. Eisenberg, Supervisor
Special Projects Unit
Materials and Processes Laboratories

Approved by:

G. V. Browning
Manager
Materials and Processes Laboratories

Unless otherwise expressly restricted on the face of this document, all use, disclosure, and reproduction thereof, by or on behalf of the government, is expressly authorized. The recipient of this document, if other than government of the United States of America, shall not duplicate, use, or disclose, in whole or in part, the information disclosed herein, except for, or on behalf of this government and to fulfill the purpose for which this document was delivered to him by the government.

PROCESS TECHNIQUES STUDY OF INTEGRATED CIRCUITS

Quarterly Report No. 4

INTRODUCTION

The present report follows, with minor exceptions, the format of the previous quarterly report. A new section in this report (Item 2-C) discusses electron paramagnetic resonance spectrometry of oxidized silicon. This investigation, as originally proposed, should lead to an estimation of unfilled atomic orbitals (silicon vacancies) in the vicinity of the Si/SiO_2 interface. Positive identification of such states should provide presumptive evidence for oxygen vacancies whose participation in inversion phenomena has been inferred in the past. Identification of such states does not prove their mobility under inversion conditions but constitutes a necessary first step in developing the analytical tools required for such proof. In any event, the investigation will contribute to a more detailed understanding of the molecular structure of the silicon dioxide layer, particularly at the region of the substrate interface.

The section on gas ambient effects (Item 1-B) has been expanded to include work on the high temperature effects of hydrogen in addition to those produced by polar gases at low temperature.

Investigation of the effects of contaminated water on dielectric defect incidence (Item 2-D) has been terminated because of the absence of any observable effect due to mechanical carry-over. It is concluded that deionized water vaporized by the oxygen input stream exceeds the minimum purity required for preventing dielectric defects from this source.

ACCOMPLISHMENTS

Item 1

A. Tool Damage Effects

Crystal damage arising from various tooling processes, such as scribing and breaking, normally is prevented from penetrating device structures by providing sufficient dead area between devices to accommodate such effects. Little analytical attention, however, has been focused on possible longer range effects not excluded by this measure. Type of possible crystal damage exist in considerable variety. Crystal imperfections may be classified according to the method of Van Bueren[1] into zero, one, two, and three dimensional faults as summarized below:

1. Zero Dimensional or Point Defects
   a. Vacancies
   b. Interstitials
   c. Substitutional impurities
2. One Dimensional or Line Imperfections

   Dislocations
3. Two Dimensional or Surface Imperfections
   a. 1st order twin - nearest neighbor relations satisfied 2nd nearest neighbor relations not satisfied
   b. Stacking fault - complimentary pair of twins returning to original orientation one or two layers wide
   c. Microtwins - essentially stacking faults which are hundreds of layers in width
   d. Subgrain boundaries - periodic dislocations - slight misorientation of blocks - blocks can have any size
   e. The heteroepitaxial interface between phases or materials is a special case of the subgrain boundary.

f. Higher order twinning - twinned areas bear a definite relationship to the matrix, but boundaries are noncoherent.

g. Grain boundaries - boundaries noncoherent - a general preferred orientation may exist. If grain size is small and orientation perfectly random, the crystal is polycrystalline.

h. Amorphous material - random orientation - grain size < 500 Å

4. <u>Three Dimensional or Volume Imperfections</u>

a. Voids

b. Inclusions

Most methods of detecting and characterizing crystal defects utilize the fact that a perfect crystal acts as a three dimensional diffraction grating[2]. The interaction of electromagnetic radiation with the grating produces measurable diffraction effects which are directly related to the crystal perfection. The measurements are made with precision goniometers, photographic film, and scintillation detectors or geiger counters with chart recorders.

1. <u>X-Ray Diffraction</u>

a. Rocking curve measurements using a double crystal x-ray spectrometer - useful for measuring dislocation densities of 10^7 to 10^9 lines per cm^2.

b. Laue back reflection - grain orientation differences of >6 minutes of arc with grain size of >100 microns. Strain in the crystal is manifested in asterism or spreading of the diffracted spots.

c. Diffraction contrast topography:

(1) The Shultz technique brings out grain boundaries of >15 seconds of arc.

(2) Lang and Berg-Barrett techniques show subgrain boundaries and dislocations from 10 to 10^7 lines per cm^2. Strain, twins, voids, inclusions can all be detected.

d. Three circle goniometer measurements using x-ray Bragg diffraction. This technique is particularly valuable in determination of orientation relationships between single crystal films and their substrates. The existence of microtwinning, the twinning planes, and the extent (percent of total volume) of the twinning in amounts greater than ½ to one percent can be detected.
e. Debye-Sherrer powder patterns for determination of composition, phase of polycrystalline aggregates.
f. Divergent beam x-ray photography - used for precise determination of lattice parameters. Strain and lattice contraction or dilation due to impurities can be detected in this manner.

2. Electron Diffraction

a. Transmission - useful for determining all one, two, and three dimensional crystal defects when the crystal film can be separated from the substrate and made sufficiently thin (< 2000 Å).
b. Reflection diffraction - angle of incidence, ½ to one degree; beam penetration, 50-100 Å. Used for examination of thin crystal films or crystal films which are deposited on a substrate of similar crystal structure and lattice constant, i.e., Ge on GaAs.
c. Low energy electron diffraction - primarily for determination of crystallinity and structure of surface layers from one to three monolayers in thickness.

3. Chemical or Thermal Etching

The proper selection of chemical reagent, temperature, and time will develop etch figures at sites of one, two, and three dimensional defects. The etch figures are then viewed either optically or in the electron microscope by replica microscopy.

4. Decoration

Certain impurities in proper concentrations can be caused to diffuse to defect areas in crystals forming an

atmosphere much larger than the defect itself. This atmosphere can then be detected using light or infrared transmission through the crystal.

5. Miscellaneous

There exist, depending on the crystal, many other perfection sensitive parameters such as resistivity, dielectric constant and loss, index of refraction, density, etc., all of which may be used as a measure of perfection if the functionality of the defect towards a particular property is known.

X-ray diffraction topography techniques are among the most versatile approaches to the investigation of tool damage in silicon. Important methods are:

1. Back reflection - Berg-Barrett techniques
2. Transmission - Berg-Barrett techniques
3. Anomalous transmission - Borrmann techniques

The salient features of these techniques are compared in Table I[3]. Basically, the usefulness of the technique under consideration is dependent on two factors: (1) the imperfection or dislocation density of the crystal under consideration, and (2) the product of the thickness of the crystal and its absorption coefficient.

The method of Bonse[4] has been used to examine the field of lattice distortion surrounding dislocations and compares favorably with theoretical prediction.

According to the present survey, the most practical means of investigating crystal damage is a combination of techniques including either etching or decorating procedures, transmission electron microscopy, and the version of the Lang x-ray method employed by Schwuttke. An entire wafer can be mapped in approximately five hours by the latter method as compared with about 1 cm^2 in 24 hours by other current topographic methods. The etching and/or decorating procedures are used to verify the presence of dislocations revealed by x-ray diffraction contrast and to aid in their interpretation. Diffraction contrast images are recorded at unit magnification, and resolution

TABLE I.* COMPARISONS AMONG DIFFRACTION TOPOGRAPHY METHODS FOR MAPPING INDIVIDUAL DISLOCATIONS IN CRYSTALS

Characteristic	Method		
Name	Back reflection; Berg-Barrett	Transmission scanning; Berg-Barrett	Anomalous transmission; Borrmann
Description	Back diffraction; Bragg case-diffracted beam leaves the same surface entered by the incident beam	Thin crystal transmission diffraction; Laue case-diffracted beam leaves through same surface as transmitted beam	Thick crystal; Laue case-anomalous transmission and diffraction
Sample Size Limitations	$\mu_o t > 1$**	$\mu_o t \ll 1$	$\mu_o t \gg 1$
Dislocation Density Limitations (Resolution)	$10^6/cm^2$ or less	$10^6/cm^2$ or less	$10^4/cm^2$ or less
Specimens for Useful Analysis	Thick specimens - to show grains, subgrains, and subsub grains	For slices of moderately x-ray transparent crystals with low dislocation densities Scanning oscillator technique to display dislocations in warped and strained crystal slices	Thick crystals; internal

* Taken in part from reference 3

** μ_o = linear absorption coefficient of material;
t = crystal thickness in the direction of the incident x-ray beam

within the limits of photographic enlargement is not better than about 5 microns. Transmission electron microscopy, on the other hand, gives about 500 Å resolution but is impractical for large area scanning.

The present program is organized on the basis of four types of mechanical treatment for separating dice. They are normal scribing and breaking, scribing through a thin aluminum deposit and breaking, machining with a Norton Model 311 Dicer, and electric discharge machining. The Norton machine operates essentially on a lapping principle described in detail below (Item 1-C). The electric discharge machine utilizes minute spark discharges for eroding a metallic or semimetallic substrate. The erosion contour conforms to the tool shape applied as a counter electrode. Kerf losses are equal to the width of the tooling electrode plus the length of the spark gap. Spark gaps of a few microns are achievable, and a delicately balanced servo system prevents physical contact between electrode and substrate. The Swiss manufactured Agietron is available at Autonetics for this investigation.

Samples of silicon wafers have been forwarded to Norton Co. for machining on their Model 311 dicer. The other specimens are being prepared at Autonetics for examination of damage penetration.

B. Gas Ambient Effects

Controlled environment equipment has been set up for the analysis of polar gas effects on devices at low temperature, and for polar and nonpolar gas effects at elevated temperatures. The equipment consists essentially of device chambers designed to withstand the contemplated temperature ranges, without outgassing or leakage failure, connected to appropriate vacuum and gas input feeds.

Some insight into the contribution of adsorbed species to surface leakage currents is available from the experiments of Hackerman and Kawasaki[5] on porous glass substrates. It was found that adsorption of water, methanol, acetone, and hexane produces characteristic surface currents (in the sub-nanoampere range) within a minute after exposure. The current varied with the character of the vapor and the degree of

coverage, the more polar molecules (e.g., water) producing the greater effect per mole adsorbed. Polar molecules also were found to displace less polar molecules, such as hexane.

Although these studies were aimed at the investigation of phenomena associated with wetting, adhesion, fluid flow, and some types of catalysis, they also have implications with respect to space applications of microelectronics where cold environments are readily capable of producing condensed phases on the silicon dioxide surfaces between adjacent metallizations. The results indicate that atmospheres in integrated circuit packages should be restricted to nonpolar gases, especially the less condensable ones such as hydrogen or helium. Alternatively, a final glass encapsulation analogous to the Motorola process should provide dielectric isolation of integrated circuit conductors impervious to condensates. In this case, however, the possibility of mechanical rupture at low temperature due to thermal expansion mismatch between layers should be investigated.

High temperature investigations are being focused mainly on the reversible effects of hydrogen on transistor beta's. Further definition of such effects may furnish evidence for a better understanding of semiconductor surfaces and a basis for the prediction of changes in the electrical parameters of devices with known package ambients under various package leak rates.

Results have been obtained on five npn dual chip transistors. No significant changes in beta were noted after the packages of three of the devices were punctured, allowing room air to enter. The other two packages were left sealed in their normal ambient. All five units were then subjected to a 90 H_2 - 10 N_2 (percent by volume) bake at 290C for 24 hours. The results, presented in Table II, indicate that 9 out of the 10 transistors showed increases in beta after baking.

Previous gas analyses of similar units from the same source indicated the ambient to be mainly nitrogen. However, opportunity exists for hydrogen leakage or diffusion into the sealed packages during the 290C terminal bake. Ambient analyses are being performed on units 7 and 8 to determine whether hydrogen is present in these packages. Other devices will be opened and baked in nitrogen to further isolate the noted effects.

TABLE II. EFFECT OF HYDROGEN ON TRANSISTOR BETA'S AT ELEVATED TEMPERATURE

Transistor		Beta Measurement			
No.	Side	Initial	After Opening Package	After Bake in 10 N_2 - 90 H_2 at 290C for 24 Hours	Percent Increase in Beta
3	A	500	520	520	-
	B	380	400	420	5%
4	A	240	220	280	27%
	B	260	260	300	13%
5	A	260	260	320	23%
	B	280	280	340	21%
7	A	440	-	520	18%
	B	440	-	520	18%
8	A	480	-	600	25%
	B	480	-	640	33%

C. Instrumentation and Processing Survey

A frequently important requirement in the examination of integrated circuits at various processing stages is the measurement of the physical characteristics of thin films and surfaces. Profilometers and interferometers are designed specifically for measuring topography of a surface, including step heights at film edges; and interferometers, ellipsometers, and betascopes are designed for measuring film thickness directly.

Profilometers are based on a lightly loaded small spherical probe which slides over a surface; its movement normal to the surface is sensed and may be recorded or displayed. It can measure smoothness or step height to 25 to 100 Å[6], but if there were no deformation of the surface by the probe, its 50μ-in tip would drop only 0.1 micron into a scratch one micron wide and only 100 Å into a scratch 1600 Å side, and not distinguish a crack from a shallow scratch.

Interferometers measure differences in optical path length of the two parts of a light beam separated by a partly reflecting mirror. If only one part of the beam traverses the sample film, the measured difference of optical path length between the two parts is a measure of film thickness. Singly reflecting arrangements give a precision of 1/10 to 1/20 of the wave length of light (i.e., about 200 Å) with accuracy dependent partly on applying proper corrections necessary for index of refraction and for phase shift on reflection. Films more than a wave length may be measured and their refractive indices determined by a method such as that used by Pleskin and Conrad[7] which measures phase difference as a function of angle of incidence. To measure step heights on a reflective surface, an accessory partly-reflecting plate is placed over the sample; in this case, corrections for index of refraction and varied phase shift on reflection from different materials are not involved. If the accessory plate is 90 to 95 percent reflecting, light is multiply reflected between the sample and plate, the diffraction fringes are sharpened, and measurements may be accurate to 5 to 10 Å[8]. Inexpensive instruments are available which have a precision of 25 or 30 Å[9]. The interferometer measures any small irregularity in a sample surface as well as steps at the edges of masked deposited films, and thereby gives information about flatness

and smoothness including scratch and hole depth for details wider than the wave length of light.

Transparent films thinner than a wave length may be precisely measured to a precision of 3 percent and down to a thickness of 2 Å by ellipsometry. The change in polarization of polarized light reflected from very thin films at various angles is dependent on, and a measure of, both the thickness and refractive index of the film. Because the measured numbers are not linear variables of the film thickness, corrections must be assessed and applied for the thickness of any contaminating film.

For nondestructive assessment of opaque films with no surface evidence of their thickness, it is necessary to use penetrating radiation. The betascope[10] measures scattering of beta radiation by film and substrate. The scattering power of material increases strongly with atomic number, and if there is (a) an appreciable difference in atomic number between the film and substrate, and (b) the compositions of both film and substrate are known, or standards are available, the scattered intensity can be related to a film thickness giving a measure of thickness for films from a very few microinches to several mils with a precision of a few percent. The less energetic beta emitters are used for thin films or low atomic number layers and more energetic beta rays for thicker films. The smallest area which available commercial instruments sample is about 20 mils in diameter.

A new wafer dicing machine offered by Norton Co. (Model 311 Dicer) may become competitive with conventional scribing and breaking. Cutting is achieved by the simultaneous lapping action of a series of linear, accurately parallel-ganged steel blades operating on the wafer in a reciprocating mode through an alumina slurry of 3 micron average particle size. The principle is analogous to the old wire saw; in the present adaptation, areas up to two inches wide may be covered by as many as 70 or 80 blades operating with a six inch stroke. Cutting rate through silicon is about 0.003 inch/minute at a reciprocating frequency of 80 to 100 cycles per minute. Minimum blade thickness consistent with optimum blade life is 0.0015 inch. Kerf loss is

claimed to be 0.0005 inch greater than the blade thickness, or about 0.002 inch for the minimum practical blade thickness. External damage to adjacent surfaces by slurry motion is claimed to be nonexistent, the only erosion being that produced by the rolling grits directly between blade edges and substrate.

Item 2

A. Oxide Radiotracer Experiments

Residual beta activities of the remaining 20 tritiated wafers was determined using 4-pi geometry according to the technique previously described. These results are summarized in Table III and compared with activity data on earlier samples from the same oxidation run.

TABLE III. STABILITY OF TRITIUM LABELED PASSIVATION OXIDE

Elapsed Time (Days)	Number of Samples	Average Net Beta Count/Wafer C/M	Calculated H Content ($x 10^{16}$ atoms/cc)
0	3	257 ± 59	2.7 ± 0.6
23	3	253 ± 74	2.7 ± 0.8
150	20	186.7 ± 58.8	1.96 ± 0.60*

*Corrected for radioactive H^3 decay

Loss of activity due to H^3 exchange with the environment cannot be inferred from the last entry because of the spread in results (about 33 percent). Nevertheless, a wrapper (paper) from one of the specimens was analyzed in the 4-pi counter. No evidence of H^3 exchange was detected.

Tritium activity distribution likewise was examined for internal consistency by inverting the first three wafers (of the group of 20) on the aluminzed mylar support film and recounting. Deviation of beta activity between opposite sides was found to be relatively insignificant compared to deviation between wafers, as shown in Table IV.

TABLE IV. BETA ACTIVITY VERSUS COUNTING ORIENTATION

Sample Number	Side Supported	Activity (C/M)	Average	Deviation, Percent
1	A	88	94	6
	B	100		
2	A	279	284	1.4
	B	288		
3	A	120	118	3.3
	B	114		

It was concluded from these results that significant amounts of hydrogen are retained in the oxide matrix if steam is present in the oxidation process gas, and that it does not exchange readily at room temperature with covalently bonded ambient hydrogen.

These results, and results obtained from earlier tritium tracer experiments, were presented May 3, 1966 at the Spring Meeting of the Electrochemical Society. These results (2×10^{16} H atoms/cm^3) differed significantly from those reported by Burgess and Fowkes[11] (Sprague Electric) and Burkhardt[12] (IBM), both of whom found levels around 10^{20} atoms/cm^3. Burkhardt, however, conducted his oxidation in pure tritiated steam (no oxygen diluent, no specific activity given). Fowkes claimed his results on an air oxidation ($\sim$20% O_2) which carried the tritiated water from a reservoir. The specific activity he used was claimed to be 0.1 millicurie/gram H_2O, which is somewhat surprising in view of his reported results and of the fact that our experiments required greater than 100 millicuries/gram specific activity to achieve significant count rates. Counting techniques, which require some finesse because of the low beta energies involved, were not fully explained, and no recourse to a reference standard was mentioned. In view of these considerations, it is suspected that Fowkes' results may have erred on the high side, and a value intermediate between Burkhardt's and ours would seem to be more realistic.

Tritium experiments performed on this program differed from the others in two important respects: (1) the use of a diluent gas containing at least 40 percent O_2, and (2) termination of the oxidations with a tracer-free bake at the oxidation temperature. As explained previously, these steps were taken for two reasons: (1) to approach standard processing techniques as closely as possible, and (2) to remove the possibility that van der Waals or physically adsorbed tritiated water would remain to contribute to the observed residual activities. A further variation in this technique was the utilization of one gram of carefully metered tritiated water for the entire treatment, which is estimated to have provided only about half the water concentration present in the experiment of Fowkes. These experimental techniques, all of which contributed to lower levels of bound hydrogen in the oxide, were purposely adopted to eliminate any possibility of a spurious claim to the chemical binding of hydrogen in silicon dioxide.

It was suggested in discussion following the Burgess and Fowkes presentation that electric fields developed in the oxide may prevent escape of the relatively weak beta radiations of tritium and thus contribute to low carrier gas ionization and low counting rates. This appears somewhat unlikely because the beta energy of tritium (0.018 Mev) is weak only in comparison with other beta emitters and easily exceeds the dielectric breakdown strength of an oxide layer of 5000 Å mean thickness. Furthermore, external ionic charge is swept away by the circulation of the methane carrier gas. However, this point will be checked experimentally by stripping the oxide from one side of a tritiated wafer, evaporating a gold contact on it and recounting the remaining side with the silicon electrically grounded to the counting chamber. These results will be reported as soon as they are available.

Electromigration of tritium in silicon dioxide has not yet been carried out because initial aluminizations of oxide surfaces were found to be defective. Alternative electrode systems will be employed in subsequent experiments.

B. Isotopically Labeled Inversion Study

Recycling of some deuterated transistor specimens through inversion and recovery sequences resulted in a lowering of the observed activation energies of recovery to values more closely approximating those derived for transistors unlabeled with deuterium. These results led to a complete re-evaluation of the inversion recovery kinetics for the entire group of eight transistors. Each of the evaluations required from four to eight inversions and recoveries. The thermal activation energies associated with the recoveries are presented in Table V. Results from the first treatment indicate that the deuterated values may be higher than the hydrated values, as expected, but the spread in results does not permit definite conclusions to be drawn. The activation energy of the last listed result may, in fact, be a result of a trace of sodium ion contamination rather than deuterium. Omitting this value, the remaining four deuterated samples yield an average recovery activation energy of 0.67 ± .06 ev.

TABLE V. INVERSION RECOVERY KINETICS OF HYDRATED AND DEUTERATED TRANSISTORS

Process Steam, Initial Oxidation	Thermal Activation Energy of Recovery (e.v.)		
	First Treatment	Second Treatment	Third Treatment
H_2O	0.46	0.86	
	0.54	0.50	
	0.74	0.56	
	0.58 ± 0.08	0.64 ± 0.15	
D_2O	0.56	0.72	
	0.68	0.40	
	0.70	0.74	
	0.74	0.45	
	1.29	0.82	0.55
	0.79 ± 0.19	0.60 ± 0.16	

Results from the second treatment appear to be generally more uniform between the two groups but are more erratic. Assuming that

inversion is produced by an electrochemical transport of positive ions, one must also expect a contribution from electrode processes. Discharge of such ions in the form of neutral species at the cathodic surface would tend to remove them from participation in the charge transport process. If more than one type of ion is present in the rigid SiO_2 electrolyte, their ratios should change in succeeding inversion treatments, thus introducing variations in the kinetics of inversion recovery. Moreover, the deuterium, undoubtedly present as a minor component since it was employed only in the first oxidation, should discharge and escape by normal diffusion ultimately into the can atmosphere leaving residual normal hydrogen as the major participant. The process therefore appears to be governed, as previously proposed by Collins[13], by two types of diffusion: ionic (field dependent) transport and atomic or molecular (nonfield dependent) transport through the oxide layer. Thus, the increasing spread in results and the apparent decrease in difference between the two isotopic groups with succeeding inversions can be explained. Additional evidence of these effects is indicated by the third inversion recovery treatment on the last deuterated specimen given in Table V.

If the above concept is correct, it should be possible to increase the recovery activation energy of an invertible device by prolonged cycling in a D_2O atmosphere. Experiments of this type are planned. Also envisioned is a processing step based on the previously observed "hardening" of similar transistors to further inversion after many cycles of inversion and deinversion. The proposed procedure is designed to remove inversion effects in planar devices by repeated alternate application and removal of reverse bias during a heat treatment (e.g., during burn-in). If the surface state density can be permanently reduced thereby, the treatment will be beneficial for unipolar as well as bipolar structures, permitting lower and more stable threshold voltages in MOS-FET's.

C. EPR Absorption Spectrometry

In continuation of the investigation of oxide structure, electron paramagnetic resonance experiments have been initiated on thermally

grown silicon dioxide samples. It has been proposed previously[14] that oxygen vacancies are the mobile species responsible for the charge rearrangement observed in silicon dioxide at elevated temperatures and under applied voltage. Since oxygen vacancy sites would provide unpaired electrons from the silicon atoms, observed electron spin flips in the silicon dioxide would imply the presence of oxygen vacancies. On this assumption, the observed absorption curves can then be associated with the unpaired spin population. Preliminary EPR results have shown a significant difference in the absorption curves for oxidized and unoxidized silicon.

There are many factors which can affect the EPR measurements made on the silicon dioxide samples. The impurity atoms in the unoxidized silicon for the cases of both donors and acceptors lead to uncomplicated absorption curves. After oxidation the sample has oxygen interstitials, thought[15] to be the predominant diffusing agent during oxidation and leading to acceptor states, as well as trivalent silicon and oxygen vacancies which are considered to produce donor states. These should contribute to the character of the absorption curves, along with the electron spin interactions with neighboring nuclei and the resulting local magnetic fields that alter the symmetry and lead to hyperfine splitting. Silicon is mostly (92%) Si^{28}, but the Si^{29} (4.7%) atoms, for example, have a nuclear spin of 1/2 while Si^{28} has zero nuclear spin. Thus, even the Si^{29} unpaired electron spins can interact with their nuclei and alter the absorption curve.

The silicon dioxide, from which EPR results were obtained, was thermally grown on a pulverized sample of silicon. The powder was etched in HF, rinsed with deionized water, and dried in a nitrogen stream. After exposure to dry oxygen and dry nitrogen at 1150C for 5 minutes, wet oxygen was introduced into the furnace for a period of six hours. The estimated oxide thickness grown was 13,000 Å. The silicon powder initially weighed 1.442 grams and increased 0.459 gram during the oxidation process.

The equipment used in these experiments was an X-band Varian Model 4500-10A EPR spectrometer with 100 Kh modulation. The powdered samples were put in a 3 mm diameter quartz tube, and initial experiments were performed at room temperature. The maximum sample width that will fit into the microwave cavity is one cm; however, it was found necessary to use the thinner samples because of large energy losses when the sample overextended into the electric field of the cavity.

EPR measurements were made for silicon dioxide grown on both single crystal and powdered silicon. The single crystal samples, with thermally grown oxides up to 20,000 Å thickness, gave no measurable energy absorption. The powdered silicon sample, with its much larger ratio of silicon dioxide to silicon over the single crystal, gave the absorption curve derivative shown in Figure 1. The unoxidized silicon produced a strong symmetric absorption curve of about 25 gauss width, while the oxidized sample showed an asymmetric complex curve indicative of multiple absorptions. The large signal to noise ratio with the unoxidized sample permitted a scan of 50 gauss in 10 minutes, and showed the absorption derivative curve was symmetric and without hyperfine splitting. The detected resonance absorption with the first oxidized sample was at the lower limits of detection of the equipment (Figure 1). Further improvements are possible as these results are from preliminary experiments to prove feasibility of the method.

Further experimentation will be necessary to bring out sufficient detail with oxidized samples to relate the absorption curves to oxygen vacancies. The first integral of the curves in Figure 1 will provide the energy absorbed versus the applied magnetic field, while the second integral will be a measure of the number of spin flips, which is of primary interest here.

Calculations of the spectroscopic splitting factor for these first samples are not considered very accurate because the equipment was not calibrated for that purpose in the initial searching for resonance absorption.

One g value reported[16] for phosphorus doped (10^{18} atoms/cm^3) silicon (unoxidized) in powdered form is $2.001 \pm .001$. The absorption

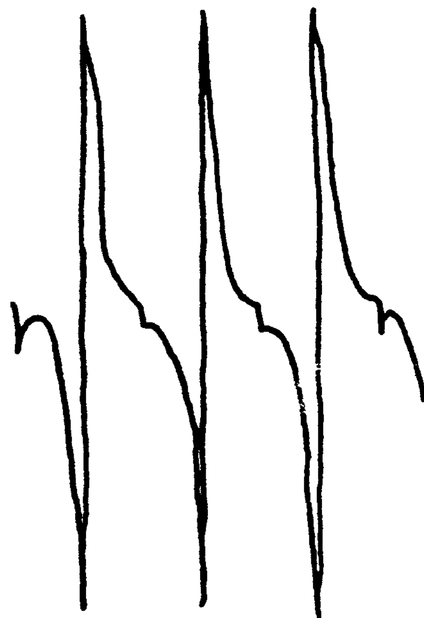

f = 9.5250 Kmh
100 gauss/inch

Unoxidised Silicon Sample

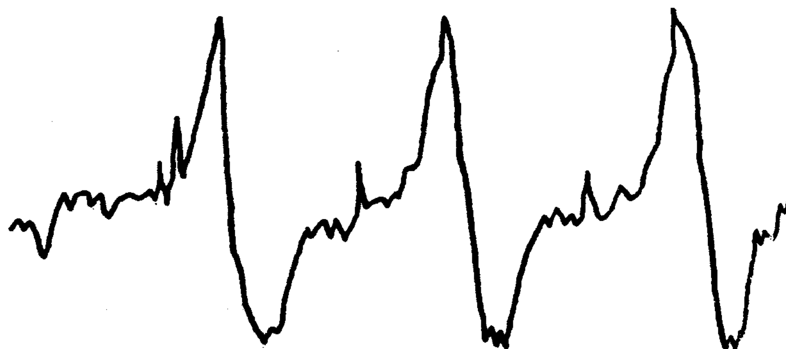

f = 9.5253 Kmh
50 gauss/inch

Oxidised Silicon Sample

FIGURE 1. EPR ABSORPTION DERIVATIVE CURVES

peak was found to be independent of temperature in the range of $4^{o}K$ to $300^{o}K$, while the line width increased from 2 g at $4^{o}K$ to 30 g at $300^{o}K$. Absorption line intensity was found to be proportional to impurity concentration.

D. Incidence of Dielectric Defects

1. Surface Preparation Studies

The effect of silicon surface preparation on the dielectric quality of thermally grown oxides is being determined. Measurements have been made on oxide layers ~1200 Å thick which have been obtained by a process similar to that currently being used by commercial producers of MOS devices to form their gate oxide. Only the silicon surface preparation varied between the five separate groups of wafers examined. The results are shown in Table VI.

TABLE VI. EFFECT OF SILICON SURFACE PREPARATION ON OXIDE DIELECTRIC QUALITY

Wafer Group	A	B	C	D	E
Surface Preparation	Chem. Polish Pre-Oxidation Cleaning	Chem. Polish Mech. Polish Chem. Polish Clean	Chem. Polish Mech. Polish HCl Etch	Chem. Polish Mech. Polish Clean	Chem. Polish Mech. Polish HCl Etch Clean
Defect Count/cm^2	213	287	228	340	266

The dielectric defects were detected by means of the previously described electrophoretic decoration test. The results indicate that a mechanical polishing step is conducive to a higher incidence of dielectric anomalies in the silicon oxide grown on the substrate. Group D, which had the mechanical polish as the final polishing step, has the highest number of defects. It can be seen from groups B and E that a chemical removal of Si

after the mechanical polish reduces the defects to some extent. However, comparison of groups C and E indicates that a solvent cleaning process following the HCl etch also increases the number of defects. The best surface preparation processes appear to be restricted to a chemical polish or a chemical-mechanical polish, followed by an HCl vapor etch. Work is continuing to verify these preliminary results.

One wafer that had not been electrophoretically decorated was selected from each group above for dielectric voltage breakdown measurements. A pattern of thirty-five 0.075 inch squares of aluminum (10,000 Å) was vacuum deposited on each of the five wafers and the voltage required to break down the silicon dioxide under each square measured. The results, which are shown in Table VII, indicate a good correlation between the oxide integrity as determined by defect count and breakdown voltage. The unmetallized silicon dioxide was found to break down at 90 volts on all five wafers, indicating a uniform thickness among these wafers.

TABLE VII. DIELECTRIC BREAKDOWN DISTRIBUTION OF WAFER GROUPS

Group	A	B	C	D	E
Number of Shorts	3	12	0	27	32
Average Breakdown Voltage	5V	3V	14V	3V	2V

Twenty additional wafers were prepared, four according to each of the five treatments above. A 12,000 Å oxide was thermally grown on the wafers. This oxide was then etched back, and the various depositions, diffusions, bakes, and oxide regrowths were made over the whole wafer, in the absence of masks, in a sequence paralleling a standard MOS process. The resulting final oxide thus approximated that for the gate region.

Since smaller aluminum dots give a more accurate distribution of breakdown voltages and capacitance minima, a pattern of 30 mil dots was vacuum deposited on these wafers, and capacitance versus voltage and breakdown voltage measurements were made. Preliminary calculations gave threshold voltages from 2 to 3.9 volts. The lowest threshold voltages were observed on wafers from group A, which also displayed the lowest dielectric defect density (Table VI). During the MOS device operation, this threshold voltage would increase slightly above 2 volts but still remain below specification, so the possibility of using a still thicker gate oxide is apparent. The breakdown voltages and their distribution across the wafer for both the metallized and unmetallized oxide are being further analyzed.

2. Oxidation Process Variables

In continuing the investigation of the process origins of dielectric defects in silicon oxide layers, an examination is being made of the effect of oxidation conditions and surface concentration of substrate dopants, upon the oxide dielectric integrity. Oxides were thermally grown in steam, wet O_2, and dry oxygen on n- and p-type epitaxial and nonepitaxial silicon substrates. As previously reported (Quarterly Report No. 3), as-grown oxide layers show a strong dependence of defect density on oxide thickness. In addition, it appears that the defect density of oxides of a particular thickness is strongly influenced by the amount of moisture in the oxidizing ambient. This variation in oxide quality with the oxidation conditions is shown in Table VIII. It is apparent from the data that oxidation in a moist ambient is beneficial to the oxide quality.

There is the possibility that part of the observed variation in defect density with oxidation conditions may be due to a difference in growth rate since the oxidation rate increases with increasing moisture content of the ambient. It is planned to grow oxides in wet N_2 in order to determine the relative importance of moisture content of ambient and growth rate on the oxide dielectric quality. This experiment will provide oxides grown in an ambient with the same moisture level as that for the wet oxygen growth,

TABLE VIII. FACTORS INFLUENCING DIELECTRIC DEFECT DENSITY

Conditions	Defect Density/cm^2			Oxide
Substrate	N-Type Epitaxial	P-Type Nonepitaxial	P-Type Nonepitaxial	Thickness
Doping Level	$N_D \approx 10^{17}$	$N_A \approx 10^{16}$	$N_A \approx 10^{19} - 10^{20}$	
Growth Ambient				
A. Dry O_2	117	123	30	3500 Å for heavily doped sample; 3850 Å other two
B. Wet O_2	38	44		3100 Å
C. Steam	18	27		3650 Å

but the growth rate will be lower because the carrier gas does not enter into the oxidation reaction.

Another significant factor observed from the data in Table VIII is that there is relatively little difference between the defect density of oxides grown on different types of substrates with the exception of the heavily boron-doped substrate. The defect density is considerably lower in the oxide grown on this heavily doped wafer than it is on lightly doped wafers.

This result, along with the beneficial effect of moist ambient oxidation, leads to the conclusion that the dielectric quality of a grown oxide is improved when there is a departure from the intrinsic or defect-free (but not necessarily strain-free) silica structure by incorporation of hydroxyl groups or boron into the silica network. These structural modifications may have the effect of reducing mechanical stress in the oxide due to mismatch between the thermal coefficients of expansion between the oxide and the substrate. It is known, for example, that a borosilicate glass has a thermal coefficient of expansion 4-5 times greater than that of pure silica. Therefore, a boron modified oxide should provide a closer match (a difference factor of about 2 instead of 10) to the thermal expansion of the silicon substrate than a pure oxide. Hydroxyl groups in the oxide also should contribute to a less rigid (or less strained) structure which may be more resistant to mechanical rupture. Measurements of the residual stress in the oxides are planned in an attempt to determine if the postulated mechanism has validity.

The above discussion raises the question: What is defect-free passivation oxide? Since the oxide structure is glassy and amorphous to x-rays, only short range order (e.g., a matrix of cyclic Si-O-Si bridging) prevails and the term, defect, cannot be used in the sense normally applied to crystalline periodicity. Thus, although pure SiO_2 may be considered defect-free (because of the absence of foreign atoms or groups), in another context (i.e., from an applications point of view) the localized mechanical stresses, unfilled atomic orbitals and greater porosity arising from the steric limitations of Si-O-Si geometry (with its semi-rigid bonding angles) give rise to localized functional defects. Such defects not only appear to provide sites for

dielectric breakdown, but probably also act as fast etching sites (stress corrosion) and as getters for contaminants. Such stress defects and vacant orbitals, as evidenced by the available data, apparently are relieved, or saturated, by the deliberate incorporation of other oxides (including hydrogen oxide) whose geometries and bond angles accommodate, to a large degree, the steric misfit inherent in the metastable amorphous silica. In particular, metallic oxides thus incorporated provide ions which are nondirectionally bonded and are therefore most efficient in relieving bond stress in the SiO_2. Of course, monovalent ions (e.g., Na, H) are capable of migrating under the influence of temperature and electric field. Consequently, some cures for dielectric problems introduce other problems of inversion and unstable MOST gate threshold voltages. In all cases the local electric fields associated with foreign ions alter the dielectric character of the oxide. Nevertheless, the defect structure of the oxide is improved thereby in terms of bond stress relief, the filling of vacant orbitals, and densification.

If the above analysis is reasonably correct, defect improving additives for oxide should be selected on the basis of minimum ionic effects and would include such materials as B_2O_3, P_2O_5, F, and N. Incorporation of boron phosphate, BPO_4, may be particularly useful because this material is isomorphous with SiO_2[17].

3. Tap Water Steam Oxidation

The effect of particulate contamination of atmospheric origin was investigated previously with inconclusive results, the observed defect density of the control being almost as high as the "contaminated" samples. On the assumption that chance contamination may have affected previous results, the system was thoroughly cleansed, and an additional control run was made. Following this, a deliberately dirty steam source (tap water) was used in the oxidation of several wafers to determine the contribution of possible mechanical carry-over from this source to oxide imperfections.

The experimental results were again inconclusive as the oxide imperfection density for the new control wafers was about $40/cm^2$, whereas the wafers made using the tap water steam source had a defect density of $20/cm^2$. This value, $20/cm^2$, is the figure previously obtained for the control and most of the contaminated samples.

In view of these results, it is concluded tentatively that contaminations from normal filtered air and from deionized water (conditions which normally prevail in standard practice) do not make significant contributions to the incidence of dielectric defects. On the contrary, experimental evidence cited earlier suggests that the origin of dielectric defects is distinctly other than chance contamination during oxidation, and no further effort in this area is presently contemplated.

PROPOSED PLAN FOR FOLLOWING QUARTER

Crystal damage introduced by various types of dicing operations will be investigated.

Gas ambient investigations will include the reversible high temperature effects of hydrogen on transistor beta's as well as low temperature effects of polar gas adsorption on reverse current leakage.

Ionic migration in tritiated wafers will be further investigated, and beta counting technique will be further examined.

EPR spectrometry will be continued in an effort to assess the unfilled orbital population in grown oxides.

The investigation of process parameters influencing the incidence of dielectric defects will be continued.

COMPLETION INFORMATION

Approximate physical completion: 100%

Approximate expenditures: 100%

This completion applies to the original contract only. Subsequent figures will apply to the contract extension beginning May 1, 1966.

ACTION REQUIRED BY NASA

None

ACKNOWLEDGEMENTS

Contributions to the work reported herein were made by J. M. Axelrod, P. J. Besser, J. V. Brandewie, T. E. Hagey, B. T. Hogan, J. L. Kersey, and C. W. Scott.

REFERENCES

1. Van Bueren, Imperfections in Crystals, North Holland Publishing Company, Amsterdam, 1960.
2. A. R. Lang, J. Appl. Phys. 30, 1748 (1959).
3. W. W. Webb, "X-ray Diffraction Topography," Direct Observation of Imperfections in Crystals, edited by J. B. Newkirk and J. H. Wernick, Interscience Publishers, New York, 1962, p. 29.
4. V. Bonse, "X-ray Picture of the Field Distortions Around Single Dislocations," ibid., p. 431.
5. N. Hackerman and K. Kawasaki in a report on the 150th American Chemical Society National Meeting, Chemical & Engineering News, Sept. 27, 1965, p. 47.
6. N. Schwartz and R. Brown in 1961 Transactions of the 8th Vacuum Symposium and Second International Congress, Pergamon (1962) (see also Engis Equipment Company Brochure CAS-3-06A).
7. Pleskin, W. A. and Conrad, E. E., IBM Tech. Discl. Bull. 5, No. 10, March 1963, p. 6.
8. S. Tolansky, Multiple Beam Interferometry, Clarendon Press, Oxford (1948).
9. Sloan Instrument, Santa Barbara, California; Varian Å-scope, Palo Alto, California.
10. Micro-derm Thickness Indicator, Unit Process Assemblies, Inc., Woodside, New York.
11. T. E. Burgess and F. M. Fowkes, Electrochemical Society Spring Meeting, May 1-6, 1966.
12. P. J. Burkhardt, ibid.
13. F. C. Collins, J. Electrochem. Soc. 112, 786 (1965).
14. J. E. Thomas and D. R. Young, IBM Jour. Research and Devel., September 1964, p. 368.

15. A. G. Revesz, IEEE Trans. on Electron Devices, March 1965, p. 97.
16. L. S. Korniyenko and A. M. Prokhorov, Zh. Eksp. Teoret, Fiz. 36, 919, 1959.
17. W. G. Palmer, "Experimental Inorganic Chemistry," Cambridge University Press, New York, 1954, p. 200 ff.